JACS
JOURNAL OF THE AMERICAN CHEMICAL SOCIETY
Article
pubs.acs.org/JACS

# Efficient Removal of Organic Ligands from Supported Nanocrystals by Fast Thermal Annealing Enables Catalytic Studies on Well-Defined Active Phases

Matteo Cargnello,[†,†] Chen Chen,[‡] Benjamin T. Diroll,[†] Vicky V. T. Doan-Nguyen,[§] Raymond J. Gorte,[‡] and Christopher B. Murray*[,†,§]

[†]Department of Chemistry, [‡]Department of Chemical and Biomolecular Engineering, and [§]Department of Materials Science and Engineering, University of Pennsylvania, Philadelphia, Pennsylvania 19104, United States

Supporting Information

**ABSTRACT:** A simple yet efficient method to remove organic ligands from supported nanocrystals is reported for activating uniform catalysts prepared by colloidal synthesis procedures. The method relies on a fast thermal treatment in which ligands are quickly removed in air, before sintering can cause changes in the size and shape of the supported nanocrystals. A short treatment at high temperatures is found to be sufficient for activating the systems for catalytic reactions. We show that this method is widely applicable to nanostructures of different sizes, shapes, and compositions. Being rapid and effective, this procedure allows the production of monodisperse heterogeneous catalysts for studying a variety of structure−activity relationships. We show here results on methane steam reforming, where the particle size controls the $CO/CO_2$ ratio on alumina-supported Pd, demonstrating the potential applications of the method in catalysis.

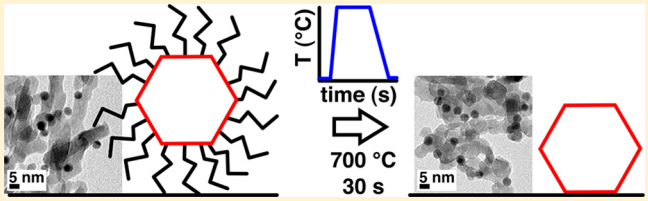


## 1. INTRODUCTION

A variety of uniform nanocrystals (NCs) and heterostructured materials with different sizes, shapes, and compositions can be prepared with nanometer precision using surfactant-assisted organic- or aqueous-based techniques.[1−3] This nanoscale control over a wide variety of different crystallographic surfaces and compositions is very appealing for catalytic studies because it allows accurate structure−activity relationships and mechanisms to be made.[4] Studying finely controlled NC systems is important for answering fundamental questions that could allow the preparation of more active catalysts.

The major drawback of colloidal synthetic methods is that they often require surface-bound surfactants to achieve colloidal stability and to control size and shape. Unfortunately, catalysis relies (in most although not all cases[5]) on having clean surfaces where reactants can bind to surface atoms and undergo chemical transformations into the desired products. Obtaining clean surfaces free of extraneous species in these uniform systems is therefore essential to prepare active, stable, and selective catalytic materials for numerous applications. It has been clearly shown that the removal of the ligands is essential for observing full activity. Even small amounts of ligands left on the surface might be extremely detrimental for catalysis.[6]

Several methods have been reported in the literature to remove organic surfactants and stabilize the surfaces of nanoparticles, small clusters, or even single atoms for catalysis.[7] The most popular ways include thermal treatments at low temperatures,[8,9] solvent extraction,[10] chemical treatments to strip the ligands off the particles,[11−13] methods involving plasma,[14] or UV-ozone cleaning procedures.[15,16] All these methods can remove organic byproducts and activate catalysts to some extent. The problem lies in the fact that more gentle approaches may leave residues that block the active sites, and harsher treatments can cause unwanted changes in the morphology of the systems and sintering of the clusters/particles that compromise their uniformity. Furthermore, some of these methods require long treatments to be effective.[17]

In previous work, we found that the minimum temperature required for removal of organic ligands and activation of group VIII metal catalysts by thermal treatments was 300 °C.[18] Despite having narrow particle-size distributions, the slow heating ramps and long annealing times led to a change in the initial particle shapes and a restructuring of the nanocrystals onto the support.[18] The reconstruction was particularly noticeable with metal nanoparticles on $CeO_2$ (ceria) support and can be explained by the propensity of metals to wet the ceria surface.[19] Reconstruction must be avoided to study size and shape effects on catalytic activity. UV-ozone is one of the best methods because it is relatively mild and it works at room temperature. However, there are reports indicating that catalysts are not completely activated following this process, likely due to incomplete removal of surface-bound surfactants.[17]

Here we report on a simple yet effective thermal treatment to remove organic ligands from catalysts prepared by colloidal

**Received:** March 30, 2015
**Published:** May 11, 2015





DOI: 10.1021/jacs.5b03333
J. Am. Chem. Soc. 2015, 137, 6906−6911

methods. We show that the uniformity of the particles is preserved while the systems are activated for catalytic reactions. We expect this method to be valuable to other materials and applications. As a demonstration of the usefulness of this approach, we present studies on methane activation through steam reforming on size-selected Pd NCs.

## 2. EXPERIMENTAL SECTION

**2.1. Synthesis of Pd Nanocrystals.** The synthesis was performed using standard air-free Schlenk techniques. Reaction conditions for appropriate sizes are reported in Table 1. 76 mg of palladium acetylacetonate (0.25 mmol, 35% Pd, Acros Organics) were dissolved in 10 mL of either trioctylamine (TOA, 97%, Acros Organics) or benzyl ether (BE, 98%, Sigma-Aldrich) together with oleylamine (OLAM, 80−90%, Acros Organics) and oleic acid (OLAC, 90%, Sigma-Aldrich), if needed. The mixture was evacuated at rt (pressure <2 mTorr) for 5 min, then trioctylphosphine (TOP, 97%, Sigma-Aldrich) was injected, and the mixture was kept under evacuation and heated to 100 °C for 30 min. The flask was then switched to nitrogen, and the yellow solution was quickly (∼50 °C $min^{-1}$) heated to the appropriate temperature and kept for 15 min. The reaction was cooled to <50 °C and open to atmosphere for purification. Particles were washed with isopropanol and separated by centrifugation (8000 rpm, 3 min) three times, with the addition of 10 μL of oleylamine after each step except after the final wash. Finally, particles were dissolved in toluene producing a deep black solution at a concentration of ∼25 mg Pd $mL^{-1}$.

**Table 1. Conditions for the Synthesis of Pd Particles Used in This Work**

| Average Pd Size | Solvent | OLAM (mmol) | TOP (mmol) | Temp (°C) |
|---|---|---|---|---|
| 2.3 | TOA | 1.25 | 0.5 | 290 |
| 3.5 | TOA | 1.25 | 2.5 | 290 |
| 4.4 | TOA | 5 | 1.25 | 290 |
| 5.5 | TOA | 5 | 2.5 | 290 |
| 7.7 | BE | 2.5 + 0.25 OLAC | 1.25 | 250 |

**2.2. Synthesis of Tetrahedral Pt Nanocrystals.** The synthesis was performed using standard air-free Schlenk techniques. 78 mg of platinum acetylacetonate (98%, Acros Organics) were dissolved in 10 mL of trioctylamine (97%, Acros Organics) together with 0.64 mL of oleylamine (80−90%, Acros Organics) and 2.5 mL of oleic acid (90%, Sigma-Aldrich). The mixture was evacuated at rt (pressure <2 mTorr) for 5 min, then 45 μL of trioctylphosphine (97%, Sigma-Aldrich) were injected, and the mixture was kept under evacuation and heated to 100 °C for 30 min. The flask was then switched to nitrogen, and the yellow solution was quickly (∼50 °C $min^{-1}$) heated to 250 °C and kept at this temperature for 30 min. The reaction was cooled to <50 °C and open to atmosphere for purification. Particles were washed with isopropanol and separated by centrifugation (8000 rpm, 3 min) three times, with the addition of 10 μL of oleylamine after each step except after the final wash. Finally, particles were dissolved in toluene producing a deep black solution at a concentration of ∼25 mg Pd $mL^{-1}$.

**2.3. Synthesis of Au@FexOy Core−Shell Structures.** The synthesis followed literature procedures.[20]

**2.4. Preparation of Catalyst Powders.** A dispersion of 1 g of either $Al_2O_3$ (TH100-150, Sasol, calcined at 900 °C for 24 h before use) or $CeO_2$ (prepared by precipitation of $Ce(NO_3)_3$ with $NH_4OH$[21] and calcined at 700 °C for 5 h) in toluene (50 mL) was sonicated for 5 min and then stirred at high speed. A solution containing an appropriate volume of Pd NCs (to give a final catalyst loading of 0.5 wt %) was prepared by diluting the NCs to 10 mL with tetrahydrofuran. This solution was then quickly added to the support dispersion in toluene and left under fast stirring for 5 min. The support became dark, and the solution was colorless at this point. The powder was recovered by centrifugation (8000 rpm, 3 min), washed once with tetrahydrofuran, and recovered by centrifugation again (8000 rpm, 3 min). The sample was finally dried in an oven at 110 °C overnight before use. This sample is considered untreated.

**2.5. Rapid Thermal Treatment of Catalyst Powders.** The untreated sample was placed in an alumina crucible. A square furnace (Thermolyne, Thermo Scientific) was preheated to an appropriate temperature (300, 500, or 700 °C), and the sample was swiftly introduced using a pair of long, heat resistant tongs (**ATTENTION: the high temperature in the furnace can cause burns, and the introduction and withdrawal of the samples must be performed carefully**). The treatment was performed in static air. After the appropriate time interval, the sample was again quickly removed from the furnace and left cooling on a benchtop.

**2.6. Characterization Techniques.** TEM was performed on a JEOL JEM 1400 operating at 120 kV and HRTEM on a JEOL JEM 2100 operating at 200 kV. Samples were prepared by drop-casting isopropanol dispersions of the samples onto 300 mesh carbon-coated Cu grids (Electron Microscopy Sciences). Particle size distributions were calculated using ImageJ software to measure particle diameter. FT-IR was performed on films of Pd NCs prepared by drop-casting of concentrated solutions onto quartz substrates; spectra were collected using a Thermo-Fisher Continuμm FT-IR system in transmission mode. Inductively coupled plasma optical emission spectrometry (ICP-OES) was performed on a SPECTRO GENESIS ICP spectrometer.

**2.7. Catalytic Characterization.** CO oxidation experiments were conducted at overall atmospheric pressure. Measurements were performed in a tubular quartz reactor (length ∼400 mm, internal diameter of 4 mm). The catalyst (20 mg) was sieved below 150 μm of grain size and loaded into the reactor to give a bed length of about 2 mm, between two layers of quartz wool used both for preventing displacement of the catalyst powder and for preheating the reagents. The reactor was heated by a Carbolite tubular furnace, and the temperature was monitored with a K-type thermocouple placed inside the furnace but on the external side of the quartz reactor. No appreciable conversion was detected when only quartz wool or the bare supports (ceria and alumina) were placed in the reactor, in the range of temperatures used for this study (under our conditions, bare ceria starts to give >1% CO conversion only above 150 °C). The reactant mixture composition, CO(1%) + $O_2$(1%), was controlled by varying the flow rates of CO, $O_2$, and He while the total flow rate was kept constant at 30 mL $min^{-1}$. The conditions corresponded to a Gas Hourly Space Velocity (GHSV) of 45 000 mL $g^{-1}$ $h^{-1}$. The composition of the effluent gases was monitored online using a Gas Chromatograph (GC) (Buck Scientific 910) equipped with a Thermal Conductivity Detector (TCD) and He as the carrier gas. Prior to measuring rates, each catalyst was reduced under a flowing mixture of $H_2$ (5%) in He at 40 mL $min^{-1}$ at 150 °C for 15 min. After the sample was cooled to room temperature, the reactant mixture was then introduced, and the reactor was heated up to the desired temperature at 3 °C $min^{-1}$.

The methane steam reforming (MSR) and water−gas shift (WGS) experiments were performed in a 1/4-in., quartz, tubular reactor, using 100 mg of catalyst. Water was introduced to the reactor by saturation of a He carrier gas flowing through deionized water. For MSR, the reactant partial pressures at the inlet were fixed at 35 Torr $CH_4$ and 70 Torr $H_2O$ with a total flow rate of 120 mL $min^{-1}$. For WGS reaction, the reactant partial pressures were fixed at 25 Torr CO and 25 Torr $H_2O$ with a total flow rate of 120 mL $min^{-1}$. In determining reaction rates, conversions of $CH_4$ or CO were kept well below 10% so that differential conditions could be assumed. Products were analyzed using an online gas chromatograph (SRI8610C) equipped with a Hayesep Q column and a TCD detector. Prior to measurements, each catalyst was pressed into thin wafers and then cleaned at 300 °C in a flowing mixture of 20% $O_2$ and 80% He for 30 min.

Pd dispersions were quantified by volumetric CO adsorption measurements at room temperature following appropriate pretreatments. The calcined samples were placed in the adsorption apparatus, heated in 200 Torr of $O_2$ at 250 °C, and then reduced at 150 °C in


DOI: 10.1021/jacs.5b03333
J. Am. Chem. Soc. 2015, 137, 6906−6911

200 Torr of $H_2$. The samples were then evacuated, cooled to room temperature, and then exposed to small pulses of CO until no further CO uptake was detected.

## 3. RESULTS AND DISCUSSION

The method consists of a rapid thermal treatment of the sample in air for a very short time with very fast heating and cooling ramps. This process is realized by introducing the sample into a furnace which had been preheated at a specific, relatively high temperature. The sample is quickly removed from the furnace after the treatment and cooled down on a benchtop. The heating and cooling ramps that can be obtained with this method are of the order of several tens of degrees per second, similar to rapid temperature annealing procedures used in the semiconductor industry for introducing dopants in silicon.[22] With these high heating and cooling ramps, kinetic transformations are favored over thermodynamics, preventing the system from relaxing to its lower energy state (e.g., by reducing high surface energy facets or surface energy in general via sintering).

We initially demonstrate that our method is effective using monodisperse 7.8 nm Pd nanocrystals (Figure S1). The nanocrystals were prepared by thermal decomposition of organometallic precursors in the presence of surfactants.[18] The particles were drop-cast onto a quartz slide and subjected to thermal treatments using different heating programs. Infrared spectroscopy was employed to evaluate the degree of removal of organic ligands by looking at the C−H stretching region of the spectrum (3000−2700 $cm^{-1}$), which is free of other signals in nanocrystals (Figure 1). At 300 °C, about 10 min were needed to bring the C−H stretching signal to below 95% of the initial intensity. By treating the particles at 500 °C for only 60 s, the C−H signals disappear, indicating complete removal of the organic ligands. At a temperature of 700 °C, the removal is complete in the even shorter period of 30 s.

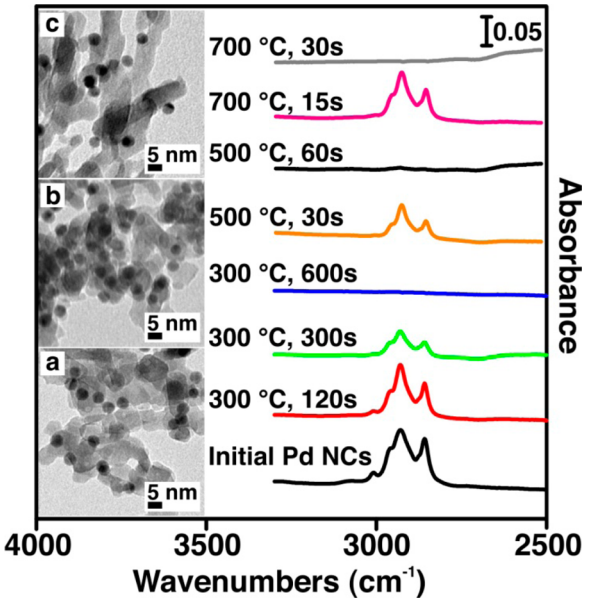


**Figure 1.** FT-IR studies of different treatments applied to Pd nanocrystals. The particles were drop-casted onto a quartz slide, introduced into a preheated furnace at the indicated temperatures, and heat-treated for the indicated period of time. The powder samples were subjected to the same treatment, and representative TEM pictures are reported in insets a (300 °C, 600 s), b (500 °C, 60 s), and c (700 °C, 30 s).

Size-distribution histograms of the initial Pd NCs and of the supported NCs treated at different temperatures are reported in Figure 2. The average particle size of the initial Pd NCs is 7.8 ± 0.5 nm. After removal of the ligands at 300, 500, or 700 °C, the size shows only a very small change to 7.6 nm and the variation remains below 6%. It should be noted that, when using rapid thermal annealing procedures but with slower heating ramps (on the order of 100−300 °C $min^{-1}$), particle size distributions are not as narrow as when using the above-described temperature-shock treatment.

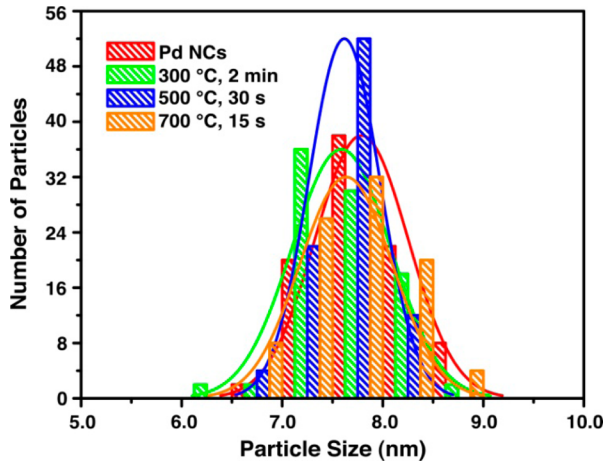


**Figure 2.** Histograms of particle size distributions for the initial Pd NC sample and for the supported systems treated at different temperatures and times. Lines represent Gaussian fittings of the distributions.

To demonstrate the wide applicability of our method, we investigated the effect of the rapid thermal treatment onto particles with different morphologies and shapes. Au@$Fe_xO_y$ core−shell particles and tetrahedral Pt NCs were heat-treated at 500 °C for 60 s to remove the organic surfactants. Representative TEM pictures (Figure 3) demonstrate that the geometry and shape of the NCs are maintained. The Au@$Fe_xO_y$ NCs, in particular, show a shrinkage in the shell volume (the void space between the Au and iron oxide shell is drastically reduced after the treatment), demonstrating that the thermal treatment was responsible for increasing the density of the shell surrounding the Au core. In the case of Pt, there is no appreciable difference in the morphology of the NCs after the treatment, with sharp edges and round corners present in both samples. This is an important result considering that clean, tailored facets of a particular crystallographic orientation are very interesting for fundamental catalytic studies.[23] It is also likely that a thermal treatment does not introduce surface disorder as is generally the case for UV-ozone procedures.[24]

The removal of the ligands with the present rapid thermal procedure not only maintains the narrow size distribution of the particles, their shape and composition but also activates the systems for catalytic reactions. It is indeed important to keep in mind that, despite IR suggests the removal of ligands has taken place, the catalytic activity is the final proof that the method is effective. We therefore demonstrate that the removal of the organic ligands leads indeed to the full activation of catalysts by using CO oxidation. CO oxidation by Pd/$CeO_2$ occurs at temperatures much below those which have been found to remove organic ligands[18] and therefore provides a gauge of the


DOI: 10.1021/jacs.5b03333
J. Am. Chem. Soc. 2015, 137, 6906−6911

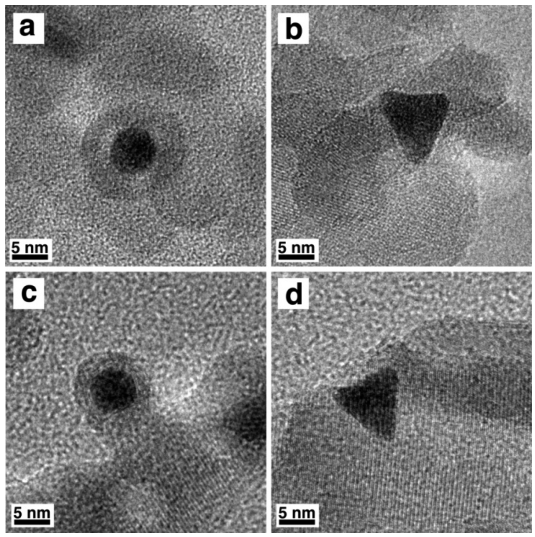


**Figure 3.** Representative TEM images of Au@$Fe_xO_y$ core–shell structures (a, c) and tetrahedral Pt NCs (b, d) before (top) and after (bottom) fast thermal treatment at 500 °C for 60 s. The NCs maintain their size and shape; only a modest shrinkage in the shell volume is observed for Au@$Fe_xO_y$.

efficacy of our annealing strategy. Pd/$CeO_2$ was chosen because this catalyst shows activity at lower temperatures compared to other supported systems.[18] Light-off curves of CO oxidation experiments provide qualitative results of the effectiveness of the ligand removal (Figure 4). It is found that the untreated

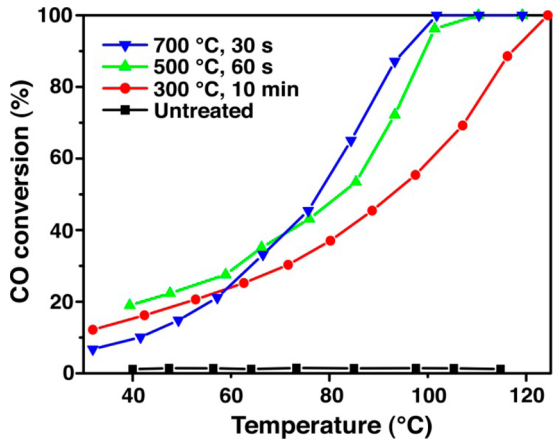


**Figure 4.** CO conversion as a function of temperature for a Pd/$CeO_2$ sample that was untreated (organic ligands are still on the surface of the particles) or rapidly heated to 300, 500, or 700 °C as indicated.

sample is not active for CO oxidation in the investigated temperature window, but after removal of the organic ligands by treatment at 300, 500, or 700 °C, the catalyst is activated. Surface blockage by the ligands is the cause for the observed inactivity of an untreated sample, given that even by reducing the catalyst in situ before reaction did not produce any appreciable CO conversion activity in the investigated temperature window.

Given that the uniformity of the particles is maintained after the ligand removal at high temperature, we investigated the influence of particle size on a reaction that occurs under conditions at which low-temperature treatments would not provide useful data, such as methane steam reforming (MSR). The activation of methane for this reaction occurs at temperatures above 300 °C, requiring active and thermally stable systems.[25] Pd NCs in five different sizes ranging from 2.3 to 7.7 nm and narrow particle size distributions were prepared and deposited on $Al_2O_3$ and $CeO_2$ supports (Figure S2). The ligands were removed and the catalysts activated at 700 °C for 30 s, as described above. CO chemisorption studies (Table 2)

**Table 2. TEM and CO Chemisorption Characterization of Pd/$Al_2O_3$ Samples after Thermal Treatment at 700 °C for 30 s**

| Pd particle size (nm)[a] | Pd dispersion (%)[b] | Pd particle size (nm)[b] |
|---|---|---|
| 2.3 ± 0.2 | 49 | 2.3 |
| 3.5 ± 0.2 | 33 | 3.4 |
| 4.4 ± 0.3 | 26 | 4.3 |
| 5.5 ± 0.3 | 20.3 | 5.5 |
| 7.7 ± 0.5 | 16 | 7.0 |

[a]Calculated from TEM. [b]Calculated from CO chemisorption experiments assuming a spherical geometry and a CO/Pd stoichiometry of 1. Dispersion is defined as the ratio of Pd atoms able to adsorb CO divided by the total number of Pd atoms.

show an increased Pd dispersion at decreasing Pd particle size in the series, corroborating the TEM studies that demonstrate that particle size and size distribution are well maintained. Furthermore, chemisorption data of the alumina-supported samples demonstrate that the surface of the Pd NCs is able to coordinate CO and is, therefore, free of ligands/contaminants, because samples are capable of CO uptake. The calculated particle diameter by CO chemisorption, assuming a spherical geometry,[26] is in very good agreement with TEM studies, except for a slight deviation in the 7.7 nm sample, for which the small volume of CO adsorbed increases the error of the measurement. The good agreement suggests that the spherical geometry is maintained, in contrast to low-temperature treatments that tend to promote particle reconstruction.

We studied the methane steam reforming (MSR) reaction at temperatures below 500 °C, using a steam-to-carbon ratio of 2. Under these conditions, the metal dispersion was stable even for the smallest particle sizes, as confirmed by CO chemisorption experiments before and after reactivity tests. Kinetic data for this reaction are reported in Figure 5.

MSR rates for Pd/$CeO_2$ are ∼5 times higher than those for Pd/$Al_2O_3$ (Figure 5a) thanks to ceria assisting water activation and favoring the removal of activated carbon species (C*) from the Pd surface.[27−30] A larger effect on the relative rates might be expected, but the relatively high calcination temperature required for stabilizing the ceria support (700 °C) is known to reduce its surface area and alter its structure in a manner known to strongly suppress the MSR activity of Pd catalysts.[28] The data normalized by mass of accessible Pd (Pd dispersion; see Table 2) show that the reaction is size-insensitive on Pd/$CeO_2$ in the size regime of this study, and it is only weakly sensitive in the case of Pd/$Al_2O_3$, with larger particles delivering ∼4 times higher rates than smaller ones. This result is in accordance with recent studies on Pd[31] and underlines the peculiar behavior of this metal compared to others, which show a linear dependence of TOFs on exposed metal atoms.[31,32]

CO selectivity data (Figure 5b), measured at similar $CH_4$ conversion, show support and size-dependent results. To understand the selectivity data it is important to note that


DOI: 10.1021/jacs.5b03333
J. Am. Chem. Soc. 2015, 137, 6906−6911

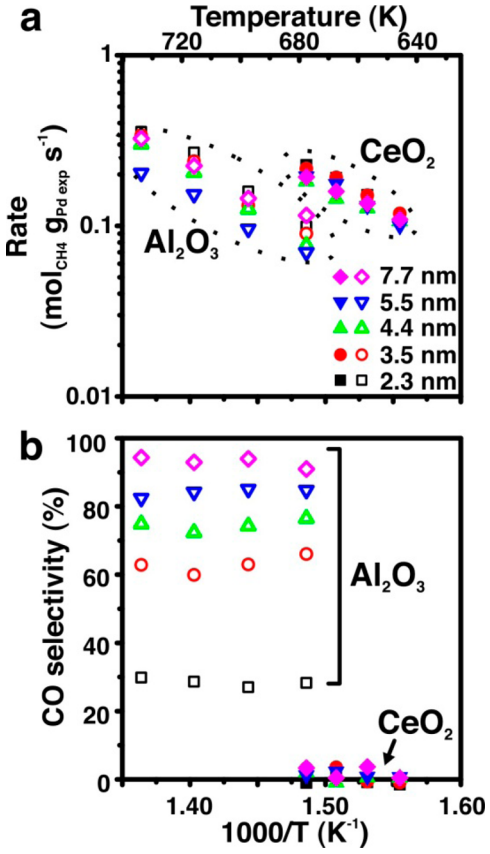


**Figure 5.** Kinetic data (a) and CO selectivity (b) for methane steam reforming reaction on size-selected Pd NCs on alumina (empty symbols) and ceria (filled symbols) after thermal treatment at 700 °C for 30 s. Carbon balance was very close to 100%. Rates were calculated by exposed Pd surface area measured by CO chemisorption.

MSR occurs under conditions that allow the water–gas shift reaction (WGSR) to occur simultaneously (Scheme 1).

**Scheme 1. Methane Steam Reforming (MSR) and Water–Gas Shift Reaction (WGSR) and Associated Reaction Enthalpy Values at 298 K**

$$CH_4 + H_2O \rightleftharpoons CO + H_2 \text{ (MSR)}$$

$$\Delta H^0_r\,(298\text{ K}) = +206\text{ kJ mol}^{-1}$$

$$CO + H_2O \rightleftharpoons CO_2 + H_2 \text{ (WGSR)}$$

$$\Delta H^0_r\,(298\text{ K}) = -41\text{ kJ mol}^{-1}$$

$CeO_2$-supported systems produce $CO_2$ (and $H_2$, not reported) almost exclusively, and only small traces of CO are measured. Because of the WGSR equilibrium, CO can be further oxidized to the formation of $CO_2$ and additional $H_2$ (Scheme 1). WGSR is known to be promoted on ceria-supported systems compared to alumina.[33] The case of Pd/$Al_2O_3$ is radically different. CO selectivity is ~30% for 2.3 nm particles, and it is similar in the temperature window of our experiments. However, with an increase in particle size, a steady increase in CO selectivity is observed, with 7.7 nm particles resulting in ~95% selectivity for CO with only trace $CO_2$ measured. In contrast to other transition metals, the high activity of Pd in C–H bond activation renders this step for MSR reversible, whereas $H_2O$ activation and WGSR steps remain irreversible.[31] For this reason, WGSR controls the equilibria of CO, $CO_2$, $H_2$, and $H_2O$ and the rates of formation of all products. We separately investigated the rates for WGSR on Pd/$Al_2O_3$ (Figure S3) and found that indeed smaller particles are more active than larger ones. Therefore, we postulate that smaller Pd particles supported on $Al_2O_3$, rich in undercoordinated metal atoms, promote WGSR and the production of $CO_2$. Larger particles instead contain a much lower fraction of undercoordinated sites, thus showing a much lower WGSR activity. It is important to note that particle size is only very slightly influenced by the reaction conditions, and narrow size distributions are still maintained despite the high temperature of the MSR (Figure S4). In this way, we demonstrate that it is possible to control the activity and selectivity of the MSR by controlling the Pd particle size on an inert support such as alumina. This result is possible by using a combination of size-selected NCs as the active phase and the appropriate activation of the catalysts by ligand removal using the method developed in this work.

## 4. CONCLUSIONS

In summary, we demonstrated that a rapid thermal treatment of supported metal nanocrystals in air is able to remove organic ligands and activate materials for catalytic reactions without changing the size, size distribution, or morphology of the supported particles. This method is widely applicable and provides a simple yet convenient way to obtain uniform catalysts that can provide fundamental insight into the reactivity of nanoscale surfaces.

## ■ ASSOCIATED CONTENT

### Supporting Information

Additional supplementary figures. The Supporting Information is available free of charge on the ACS Publications website at DOI: 10.1021/jacs.5b03333.

## ■ AUTHOR INFORMATION


### Corresponding Author

*cbmurray@sas.upenn.edu

### Present Address

†Department of Chemical Engineering and SUNCAT Center for Interface Science and Catalysis, Stanford University, Stanford, CA 94305 (USA).


### Notes

The authors declare no competing financial interest.

## ■ ACKNOWLEDGMENTS

M.C. acknowledges support from the National Science Foundation through the Nano/Bio Interface Center at the University of Pennsylvania, Grant DMR08-32802. C.C. and R.J.G. were supported by the Department of Energy, Office of Basic Energy Sciences, Chemical Sciences, Geosciences and Biosciences Division, Grant No. DE-FG02-13ER16380. C.B.M. is grateful for the support of the Richard Perry University Professorship.

## ■ REFERENCES

(1) Park, J.; Joo, J.; Soon, G. K.; Jang, Y.; Hyeon, T. *Angew. Chem., Int. Ed.* **2007**, *46*, 4630.
(2) Carbone, L.; Cozzoli, P. D. *Nano Today* **2010**, *5*, 449.
(3) Park, J.; Lee, E.; Hwang, N. M.; Kang, M.; Kim, S. C.; Hwang, Y.; Park, J. G.; Noh, H. J.; Kim, J. Y.; Park, J. H.; Hyeon, T. *Angew. Chem., Int. Ed.* **2005**, *44*, 2872.



DOI: 10.1021/jacs.5b03333
*J. Am. Chem. Soc.* 2015, 137, 6906–6911

(4) Cargnello, M.; Fornasiero, P.; Gorte, R. J. *ChemPhysChem* **2013**, *14*, 3869.
(5) Marshall, S. T.; O'Brien, M.; Oetter, B.; Corpuz, A.; Richards, R. M.; Schwartz, D. K.; Medlin, J. W. *Nat. Mater.* **2010**, *9*, 853.
(6) Wu, Z.; Jiang, D. e.; Mann, A. K. P.; Mullins, D. R.; Qiao, Z. A.; Allard, L. F.; Zeng, C.; Jin, R.; Overbury, S. H. *J. Am. Chem. Soc.* **2014**, *136*, 6111.
(7) Li, W. Z.; Kovarik, L.; Mei, D.; Engelhard, M. H.; Gao, F.; Liu, J.; Wang, Y.; Peden, C. H. F. *Chem. Mater.* **2014**, *26*, 5475.
(8) Menard, L. D.; Xu, F.; Nuzzo, R. G.; Yang, J. C. *J. Catal.* **2006**, *243*, 64.
(9) Ma, G.; Binder, A.; Chi, M.; Liu, C.; Jin, R.; Jiang, D.; Fan, J.; Dai, S. *Chem. Commun.* **2012**, *48*, 11413.
(10) Lopez-Sanchez, J. A.; Dimitratos, N.; Hammond, C.; Brett, G. L.; Kesavan, L.; White, S.; Miedziak, P.; Tiruvalam, R.; Jenkins, R. L.; Carley, A. F.; Knight, D.; Kiely, C. J.; Hutchings, G. J. *Nat. Chem.* **2011**, *3*, 551.
(11) Kilmartin, J.; Sarip, R.; Grau-Crespo, R.; Di Tommaso, D.; Hogarth, G.; Prestipino, C.; Sankar, G. *ACS Catal.* **2012**, *2*, 957.
(12) Gordon, T. R.; Cargnello, M.; Paik, T.; Mangolini, F.; Weber, R. T.; Fornasiero, P.; Murray, C. B. *J. Am. Chem. Soc.* **2012**, *134*, 6751.
(13) Elliott, E. W.; Glover, R. D.; Hutchison, J. E. *ACS Nano* **2015**, *9*, 3050.
(14) Cademartiri, L.; Ghadimi, A.; Ozin, G. A. *Acc. Chem. Res.* **2008**, *41*, 1820.
(15) Chen, W.; Kim, J.; Sun, S.; Chen, S. *Phys. Chem. Chem. Phys.* **2006**, *8*, 2779.
(16) Aliaga, C.; Park, J. Y.; Yamada, Y.; Lee, H. S.; Tsung, C. K.; Yang, P.; Somorjai, G. A. *J. Phys. Chem. C* **2009**, *113*, 6150.
(17) Li, D.; Wang, C.; Tripkovic, D.; Sun, S.; Markovic, N. M.; Stamenkovic, V. R. *ACS Catal.* **2012**, *2*, 1358.
(18) Cargnello, M.; Doan-Nguyen, V. V. T.; Gordon, T. R.; Diaz, R. E.; Stach, E. A.; Gorte, R. J.; Fornasiero, P.; Murray, C. B. *Science* **2013**, *341*, 771.
(19) Farmer, J. A.; Campbell, C. T. *Science* **2010**, *329*, 933.
(20) Cargnello, M.; Diroll, B. T.; Gaulding, E. A.; Murray, C. B. *Adv. Mater.* **2014**, *26*, 2419.
(21) Cargnello, M.; Montini, T.; Polizzi, S.; Wieder, N. L.; Gorte, R. J.; Graziani, M.; Fornasiero, P. *Dalton Trans.* **2010**, *39*, 2122.
(22) *Rapid Thermal Processing: Science and Technology*; Fair, R. B., Ed.; Academic Press Inc.: San Diego, CA, 1993.
(23) Crespo-Quesada, M.; Yarulin, A.; Jin, M.; Xia, Y.; Kiwi-Minsker, L. *J. Am. Chem. Soc.* **2011**, *133*, 12787.
(24) Vidal-Iglesias, F. J.; Solla-Gullón, J.; Herrero, E.; Montiel, V.; Aldaz, A.; Feliu, J. M. *Electrochem. Commun.* **2011**, *13*, 502.
(25) Rostrup-Nielsen, J. R.; Sehested, J.; Nørskov, J. K. *Adv. Catal.* **2002**, *47*, 65.
(26) Lear, T.; Marshall, R.; Lopez-Sanchez, J. A.; Jackson, S. D.; Klapötke, T. M.; Bäumer, M.; Rupprechter, G.; Freund, H. J.; Lennon, D. *J. Chem. Phys.* **2005**, *123*, 174706.
(27) Feio, L. S. F.; Hori, C. E.; Damyanova, S.; Noronha, F. B.; Cassinelli, W. H.; Marques, C. M. P.; Bueno, J. M. C. *Appl. Catal., A* **2007**, *316*, 107.
(28) Craciun, R.; Shereck, B.; Gorte, R. J. *Catal. Lett.* **1998**, *51*, 149.
(29) Craciun, R.; Daniell, W.; Knözinger, H. *Appl. Catal., A* **2002**, *230*, 153.
(30) Wang, X.; Gorte, R. J. *Appl. Catal., A* **2002**, *224*, 209.
(31) Yamaguchi, A.; Iglesia, E. *J. Catal.* **2010**, *274*, 52.
(32) Jones, G.; Jakobsen, J. G.; Shim, S. S.; Kleis, J.; Andersson, M. P.; Rossmeisl, J.; Abild-Pedersen, F.; Bligaard, T.; Helveg, S.; Hinnemann, B.; Rostrup-Nielsen, J. R.; Chorkendorff, I.; Sehested, J.; Nørskov, J. K. *J. Catal.* **2008**, *259*, 147.
(33) Bunluesin, T.; Gorte, R. J.; Graham, G. W. *Appl. Catal., B* **1998**, *15*, 107.


DOI: 10.1021/jacs.5b03333
*J. Am. Chem. Soc.* 2015, 137, 6906−6911